

Magnetic hysteresis and flux creep of melt-powder-melt-growth $\text{YBa}_2\text{Cu}_3\text{O}_7$ superconductors

P. J. Kung,* M. P. Maley, M. E. McHenry,* J. O. Willis, and J. Y. Coulter

Superconductivity Technology Center, Los Alamos National Laboratory, Los Alamos, New Mexico 87545

M. Murakami and S. Tanaka

Superconductivity Research Laboratory, International Superconductivity Technology Center,

1-10-13 Shinonome, Koto-Ku, Tokyo 135, Japan

(Received 16 April 1992)

Magnetic hysteresis and flux creep characteristics in melt-powder-melt-growth $\text{YBa}_2\text{Cu}_3\text{O}_7$ with Y_2BaCuO_5 inclusions were measured between 5 and 80 K for magnetic fields up to 5 T. The critical magnetization current densities which were calculated using the Bean model and the sample dimension show a weak dependence on magnetic field. The J_c values are of the order of 10^4 A/cm² at 60 K over the investigated field range. The magnetic relaxation rate $Q = -dM/d \ln t$ first drops monotonically with increasing temperatures and then gradually saturates, which is similar to the behavior of the initial magnetization M_0 versus temperature. The normalized relaxation rate $S = d \ln M / d \ln t$, plotted as a function of temperature, shows a maximum at around 30 K, and the corresponding values of S and T at the maximum are field dependent. A scaling relationship $U_{\text{eff}}(J, H) = U_i G(T) F(J/J_i) / H^{0.55}$, where $G(T) = 1 - (T/T_x)^2$, $F(J/J_i) \sim (J/J_i)^{-n}$, and U_i and J_i are scaling constants, is proposed to fit the creep data from which a universal curve is attained. The characteristic temperature T_x for the scaling function $G(T)$ is determined from the irreversibility line. The current-dependent behavior of U_{eff} obtained from this work agrees qualitatively with the result predicted by the theory of collective flux creep and suggests a vortex-glass state at low current density.

I. INTRODUCTION

Major efforts have been made to enhance the critical current densities (J_c 's) of superconductors at liquid-nitrogen temperature (77 K) since the high- T_c oxide superconductors were discovered.¹⁻³ However, due to higher operating temperatures, shorter coherence lengths, and larger anisotropy in these materials compared with conventional superconductors, rapid flux motion, which induces dissipation in the presence of transport currents, reduces the effective J_c 's that can be maintained in the presence of a magnetic field at 77 K, and has remained a persistent problem.⁴⁻⁶ Such behavior of flux creep is generally believed to account for rapid magnetic relaxation and broad resistive transitions in these high- T_c materials. Although J_c 's of 10^6 – 10^7 A/cm² at 77 K in zero magnetic field can be obtained in thin films^{7,8} and single crystals^{9,10} of Y-Ba-Cu-O, the values of intergranular J_c of these same superconductors in polycrystalline form are dramatically reduced by weak intergranular coupling. To overcome the problem of weak coupling between grains, various processing techniques such as melt texturing and thermomechanical methods have been employed to reduce weak links through grain alignment in bulk form¹¹ and in Ag-sheathed tapes and wires,^{12,13} respectively.

The method of melt-powder-melt-growth^{14,15} (MPMG) has been shown to be effective in fabricating bulk $\text{YBa}_2\text{Cu}_3\text{O}_7$ superconductors in which grain boundaries do not act as weak links. This same technique has also proven capable of introducing a fine dispersion of

second-phase Y_2BaCuO_5 (211) particles that act as effective pinning centers and enhance J_c at elevated temperature and field. It is clearly of interest to examine the effect of this enhanced pinning upon thermally activated flux motion. In addition, use of large, well-coupled crystals allows the study of flux-creep behavior over wide ranges of temperature and current density, which facilitates comparison of results with the recent collective-pinning¹⁶ and vortex-glass¹⁷ model predictions.

The standard analysis of magnetic relaxation due to thermally activated motion of flux lines out of potential wells provided by pinning centers was developed by Anderson and Kim.^{18,19} In the presence of a transport current, the Lorentz force reduces the activation energy and thermally activated flux motion then flows preferentially down the flux gradient caused by the current. The simplest assumptions of a linear approximation gives

$$U_{\text{eff}} = U_0 - JBVa = U_0(1 - J/J_c), \quad (1)$$

where V is a correlation volume and a is the hop distance for flux bundles. U_0 is an average value for the full activation energy at low current density and, by definition, J_c is the current density that reduces U_{eff} to zero. Use of this linear approximation produces a solution of the diffusion equation for magnetic relaxation ($M \sim J$) given by²⁰

$$J(t) = J_{c0} [1 - (kT/U_0) \ln(t/\tau)], \quad (2)$$

where $1/\tau$ is a characteristic attempt frequency of the magnitude of 10^9 – 10^{12} Hz and J_{c0} is the critical current

density in the absence of thermal activation. The logarithmic form of decay is generally observed over the limited time window, 1–10 h, probed in most experiments. This has led to the widespread use of the logarithmic decay rate to characterize the behavior of magnetic relaxation and the activation energy. From Eq. (2),

$$S = -(1/M_0)(dM/d \ln t) \approx -d \ln M/d \ln t \sim kT/U_0^* , \quad (3)$$

where the parameter U_0^* , obtained from measurements of the normalized relaxation rate S , may not be simply related to the low current limit of the activation energy for more general forms for $U(J)$ than the linear relation of Eq. (1). It was pointed out by Beasley, Labusch, and Webb²¹ and recently by Xu *et al.*²² that, for a nonlinear $U(J)$, U_0^* rather represents the intercept on the activation energy axis of a line tangent to the $U(J)$ curve at the instantaneous value of J . As the magnitude of stable J values accessed decreases with increasing temperature, this can cause the intercept to rise, implying a $U_0^*(T)$ that is an increasing function of T , as observed in numerous experiments. An alternative explanation of the apparent temperature dependence of $U_0^*(T)$ has been provided by models incorporating a distribution of activation energies.²³

Recently, models based on vortex-glass and collective-pinning theories have derived inverse power-law expressions for $U(J)$ that can be generally written^{16,17}

$$U(J) = (U_0/\mu)[(J_c/J)^\mu - 1] , \quad (4)$$

where U_0 is the scale of the activation energy and the exponent μ is of order 1 for the vortex-glass model and varies with the dimensionality of the vortex lattice and with the range of J/J_c in the collective pinning models. Equation (4) leads to the “interpolation” formula for the logarithmic relaxation rate:²⁴

$$S = -T/[U_0 + \mu T \ln(t/\tau)] . \quad (5)$$

This expression predicts that S will increase approximately linearly with T at low temperature and saturate for $\mu T \ln(t/\tau) > U_0$, in agreement with many recent experimental results.²⁵ In this investigation we will employ a method of analysis of magnetic relaxation data developed by Maley *et al.*²⁶ that allows a determination of $U(J)$ to be made without prior assumptions.

II. EXPERIMENTAL DETAILS

The samples of $\text{YBa}_2\text{Cu}_3\text{O}_7$ with Y_2BaCuO_5 inclusions were prepared by the MPMG method, and the details have been described elsewhere.^{14,15} The starting composition was $\text{Y}_{1+2x}\text{Ba}_{2+x}\text{Cu}_{3+x}\text{O}_{6+d}$ with $x=0.4$. Contamination of the sample during the melting step in an alumina crucible resulted in a few at. % of Al in the sample. A thin specimen of $2.75 \times 1.25 \times 1.0 \text{ mm}^3$ was cut from the as-processed material. Back-reflection Laue photographs were taken on this sample to identify the crystal orientation. It was found that the c axis is $\sim 1.8^\circ$ and $\sim 7^\circ$ off from the angular coordinates γ and δ of the

plane normal, respectively. The sample consists of several crystals that have the same orientation, and the largest surface is approximately perpendicular to the c axis. Grain boundaries are believed not to act as weak links.¹⁵ To precisely orient the c axis with the magnetic field, which is the case for all the measurements of the magnetic properties, a special sample holder was made. T_c screening, magnetic hysteresis, and magnetic relaxation measurements were performed using a Quantum Design superconducting quantum interference device (SQUID) Model MPMS magnetometer. A scan length of 3 cm was used so as to have sufficient uniformity of the applied magnetic field.²² We first measured the magnetization versus temperature ($M-T$) curves with various applied magnetic fields. The superconducting transition temperature and the irreversibility line [i.e., $T^*(H)$], which was established from the intersection of the zero-field-cooled and the field-cooled curves, were thus obtained. Observations of magnetization hysteresis ($M-H$) loops at 10–80 K with applied fields up to 5 T were also carried out, and the critical magnetization current densities were calculated using the sample dimensions and the Bean model.

For the measurement of magnetic relaxation, the sample was cooled in zero field, the magnetic field was then applied, and the time dependence of the magnetization M was measured at constant magnetic fields of 1, 2, 3, and 4 T in the temperature range of 5–80 K. In each case the magnetic field was first raised to 5 T and then lowered to the selected value. In doing so, the field applied was always well above the lower critical field of the superconductor and also sufficient to achieve the critical state $J=J_c$, where the effective barrier to flux motion is zero, throughout the entire volume of the sample. Because the magnetic irreversibility line as a function of temperature is concave downward, a wide range of temperatures and magnetic fields was thus required to fully characterize the flux creep behavior of the crystal. A typical relaxation measurement took 6 h.

III. RESULTS AND DISCUSSION

A. Irreversibility line and magnetic hysteresis

According to the result of the zero-field-cooled diamagnetic transition in a field of 20 G applied along the c axis of the crystal, the sample exhibits a sharp transition at 93 K, which suggests that the crystal consists of nearly single-phase $\text{YBa}_2\text{Cu}_3\text{O}_7$. A Meissner effect less than 1% was observed in this sample, which implies that the crystal has good flux pinning in the mixed state. The irreversibility line obtained from the zero-field-cooled and field-cooled measurements in various magnetic fields is shown in Fig. 1 in which the data fit quite well the relation $1 - (T^*/T_c) \sim H^{2/3}$, as has been previously observed.^{5,6}

To derive the critical magnetization current density, magnetic hysteresis measurements have been performed for temperatures ranging from 10 to 80 K. Figure 2 illustrates typical features of hysteresis loops at 10 and 40 K. Using the Bean model and the sample dimensions, J_c 's were calculated from the following equation:²⁷

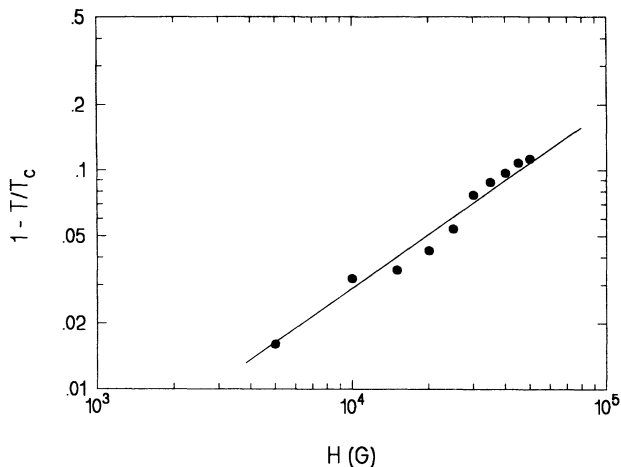


FIG. 1. Magnetic irreversibility line of the MPMG $\text{YBa}_2\text{Cu}_3\text{O}_7$ sample. Solid line is a fit to the relation $1 - (T^*/T_c) \sim H^{2/3}$.

$$J_c = 20(M^- - M^+) / a(1 - a/3b), \quad (6)$$

where M^+ (M^-) is the magnetization associated with increasing (decreasing) field, measured in emu/cm^3 , and a and b ($b > a$) are the dimensions of the rectangular cross section of the crystal normal to the applied field, measured in cm. Because a sharp Laue spot pattern with only slightly streaked features was observed, the sample is believed to have high crystalline quality, although it is multigrained. It was reported by Murakami *et al.*¹⁵ that a linear dependence of the magnetization difference ($M^- - M^+$) upon sample radius at various magnetic fields was observed experimentally, which indicates that weak links do not limit current flow in these melt-grown samples. Taking these observations into account, we use the sample dimensions to derive J_c , which should then be representative of the average superconducting properties of the specimen. As shown in Fig. 3, J_c values of the order of $10^4 \text{ A}/\text{cm}^2$ at 2 T are attained even up to 70 K. Critical current densities are almost independent of the

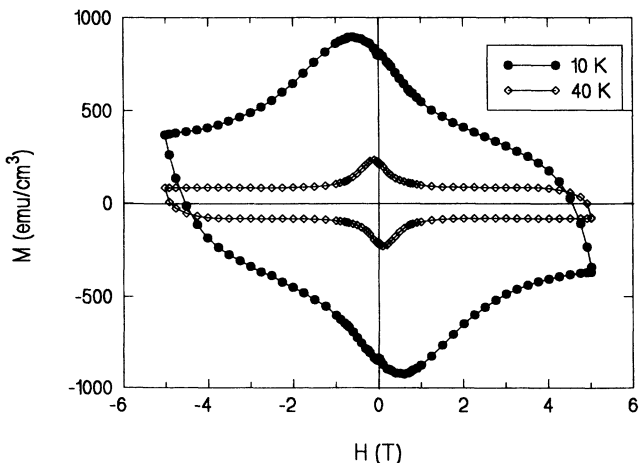


FIG. 2. Magnetization hysteresis loops with the field applied parallel to the c axis of the sample.

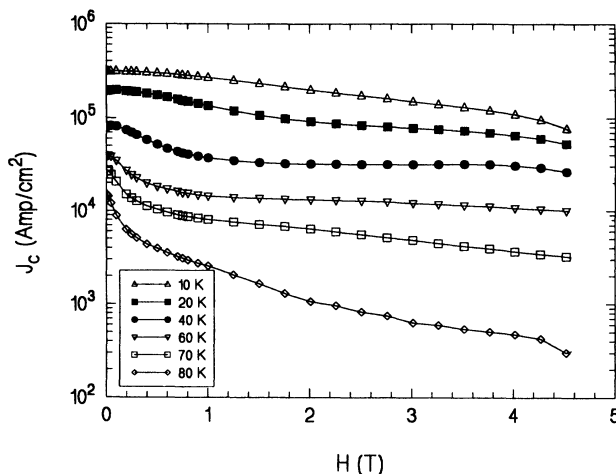


FIG. 3. Critical magnetization current densities derived from the magnetic hysteresis ($H \parallel c$ axis).

magnetic field at 30–60 K and only drop about one order of magnitude at 5 T as the temperature is changed from 20 to 70 K. Notice that for J_c 's at fields well below 1 T, the fall with temperature is not as dramatic as is usually observed in granular high- T_c bulk superconductors. These two results demonstrate both the strong intragranular pinning and the absence of weak links (strong intergranular coupling) in this MPMG processed material.

B. Magnetic relaxation

The metastability of the mixed state in the high- T_c superconductors can be experimentally demonstrated from the behavior of the logarithmic decay of the magnetization. A typical example of this linear dependence of magnetic relaxation upon the logarithm of time is shown in Fig. 4, which shows data measured at 3 T for various temperatures. For the initial transient stage, especially at high temperatures, deviations from such a linear relationship were often observed. Similar deviations near the end

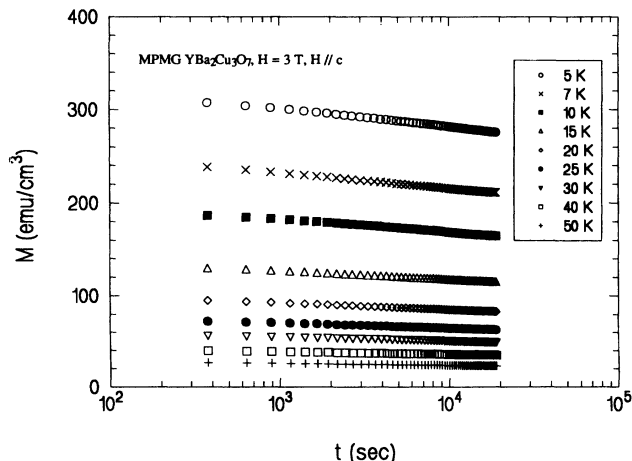


FIG. 4. Magnetic relaxation measured at 3 T, which shows the linear dependence on the logarithm of time.

of the measurement were also sometimes observed. The field dependence of the logarithmic decay rate usually decreases with increasing fields; however, logarithmic decay does not properly describe the magnetic relaxation at high temperatures and high fields. To compare the relaxation rates (Q 's) at various temperatures and magnetic fields, the Q - T - H curves are plotted in Fig. 5(a). Solid lines are guides to the eye. As can be seen, relaxation rates drop rapidly with temperature up to 30 K and decrease gradually thereafter. Such a nonlinear dependence is also observed in the M_0 , which is the initial magnetization measured just after the magnetic field is applied and the field is stable, versus temperature curves as shown in Fig. 5(b).

The curves of Q - T and M_0 - T have similar behaviors; in other words, the rate of decay depends on the magnitude of the initial magnetic moment or current density. The

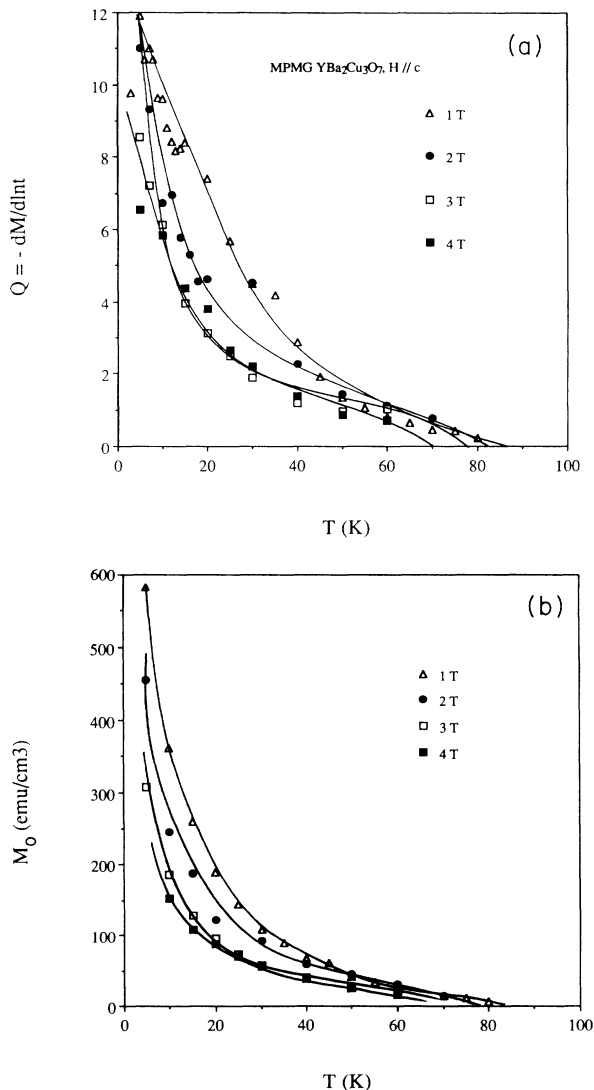


FIG. 5. The behavior of the temperature dependence of (a) the relaxation rate $Q = -dM/d\ln t$, and (b) the initial magnetization M_0 . Solid lines are guides to the eye. Notice that they both show a similar temperature dependence.

normalized relaxation rate S , which is equal to Q divided by M_0 , was extracted from the experimental data using Eq. (3). Figure 6 shows the curves of S vs T obtained from the slopes of $\ln M$ vs $\ln t$. In the range of temperatures and magnetic fields we studied, the difference in the magnitude between $(1/M_0)(dM/d\ln t)$ and $d\ln M/d\ln t$ is within 8% and the errors are less important as the temperature or magnetic field is decreased. Both curves show the same qualitative features, namely, a peak near 30 K. The peak position shifts to lower temperature when the applied magnetic field is increased, and the height of the maximum decreases slightly with field. S values fall in the range of 0.03–0.05 between 20 and 70 K in rough agreement with the “universal” plateau values noted by Malozemoff and Fisher,²⁵ but the observed slightly decreasing normalized relaxation rate with temperature above 30 K does not seem to be describable by the simple flux-creep theory [Eq. (5)]; moreover, the values tend to diverge as the temperature approaches the irreversibility line, which has also been observed in neutron-irradiated samples.²⁸ It is noted that for measurements taken only at lower temperatures this divergence will be missed.²⁹ Thus those experiments may lead to the wrong or incomplete conclusions for the temperature dependence of the normalized relaxation rate at high temperatures. The detailed behavior of S is believed to depend on the type of pinning centers (e.g., defects such as stacking faults and twin boundaries) and compositional inhomogeneity (e.g., minority phases). The prediction of the collective pinning model [Eq. (5)] exhibits the presence of only two regions: at low temperatures the term $(-T/U_0)$ yields a quasilinear response, as is observed; at high temperatures, the second term $[-\mu \ln(t/\tau)]^{-1}$ should dominate and there should be a plateau in temperature. Thompson *et al.*³⁰ have recently performed an analysis of flux-creep data (the low temperature and plateau region) on YBa₂Cu₃O₇ single crystals using this model, but the high-temperature data observed here can only be consistent with the model if μ or τ has strong im-

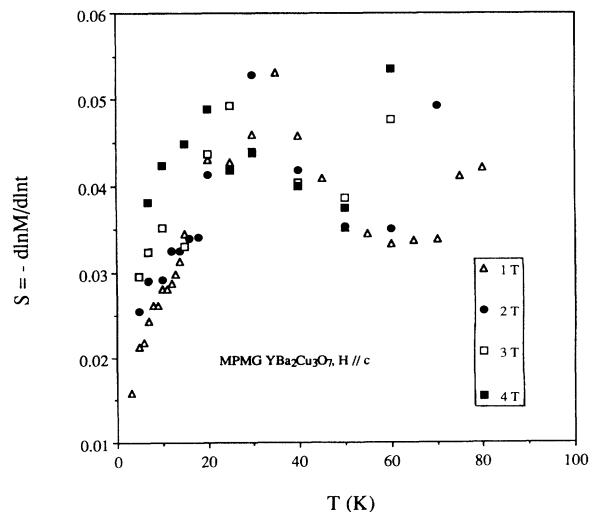


FIG. 6. Temperature dependence of the normalized relaxation rate S , which shows maxima near 30 K and diverging behavior as the temperature approaches T_c .

plit temperature (or J) dependence. Rather than explore these extensions within this somewhat limited model, we prefer to pursue a more direct approach for analyzing the flux-creep data by determining the relation between U and J directly as will be discussed in the next section.

C. Nonlinear model for $U_{\text{eff}}(J, H)$

In the preceding discussion it was pointed out that there are inconsistencies in the linear dependence of activation energy which suggests that the functional expression for U_{eff} has to be determined empirically. By considering the magnetic relaxation data and solving the diffusion equation for the local flux density, Maley *et al.*²⁶ have proposed a model to give an expression for the effective pinning energy:

$$U_{\text{eff}}/k = -T[\ln(dM/dt) - \ln(H\omega_0 a/2\pi d)], \quad (7)$$

where ω_0 is a characteristic attempt frequency, a is the hop distance, and d is the thickness of a slab of the superconductor. The effective pinning potential at a constant magnetic field can be obtained from $M(t)$ data by curve fitting the constant $C = \ln(H\omega_0 a/2\pi d)$ to give the smoothest continuous fit of the low-temperature (< 15 K) U_{eff} vs M data. To further justify such a nonlinear dependence of U_{eff} upon J , we plot $\ln(\Delta M)$ ($\sim \ln J$) vs T in Fig. 7, in which the straight lines are least-square fits

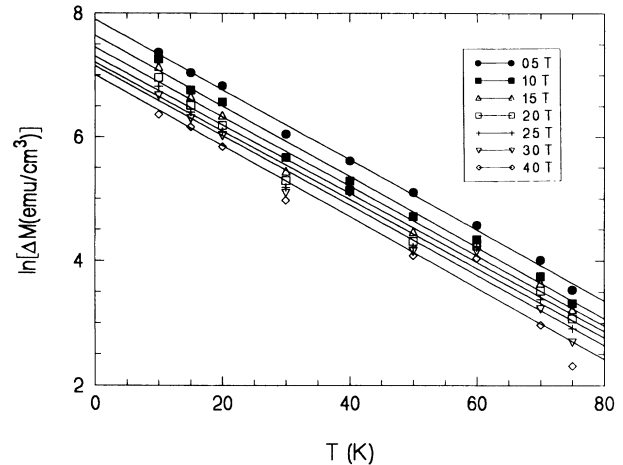


FIG. 7. The linear dependence of $\ln(\Delta M)$ vs temperature. Solid lines are least-square fits to the data.

to the data. According to Eq. (2), if the linear approach is correct, we should have a linear relationship between J and T . It is very obvious from Fig. 7 that the linear relationship between $\ln(\Delta M)$ and T indicates a nonlinear $U_{\text{eff}}-J$ dependence in this study. As shown in Fig. 8 (the upper curve of each pair), each set of data points represents a magnetic relaxation measurement performed at a fixed temperature. The C values were determined to

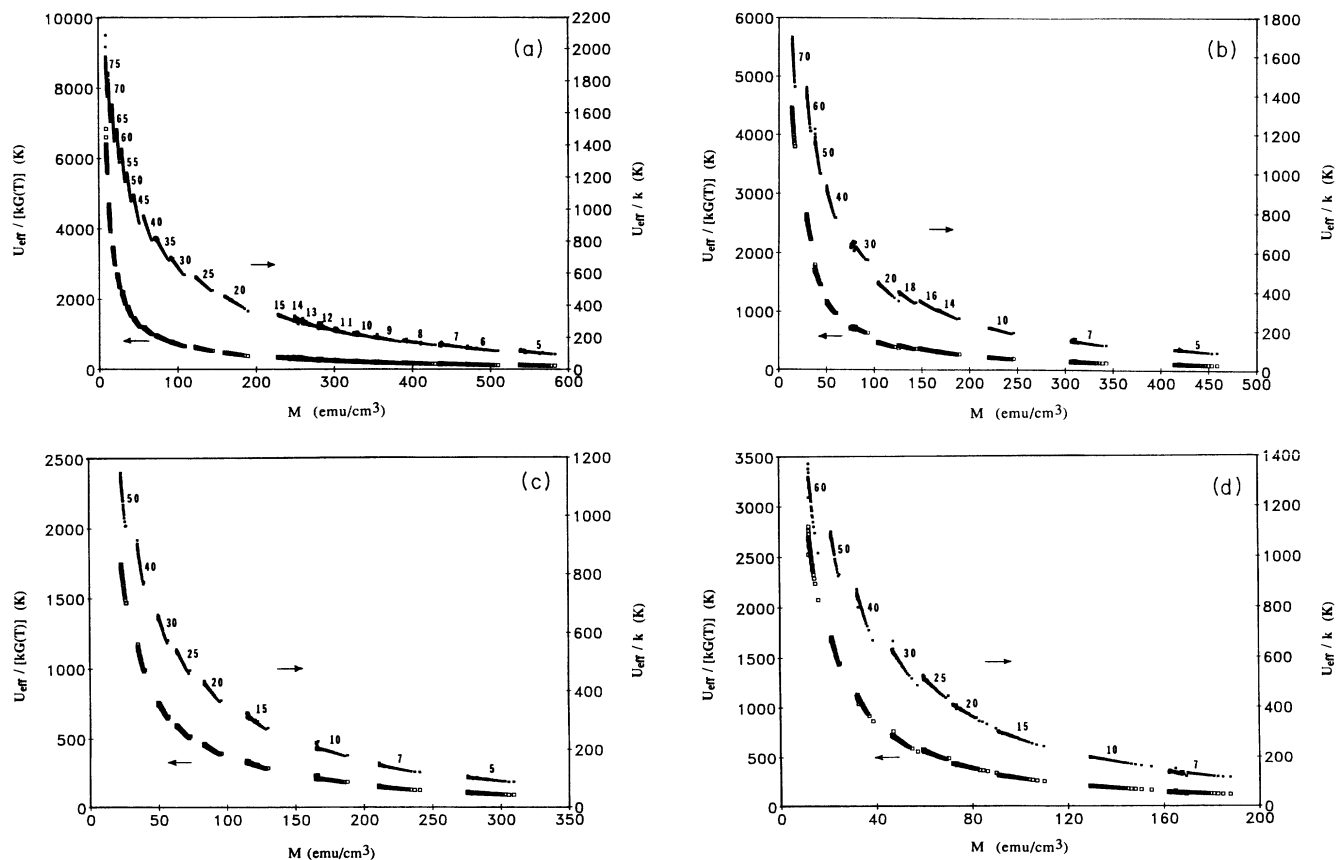


FIG. 8. Fits of the data to U_{eff}/k and $U_{\text{eff}}/[kG(T)]$ vs magnetization M at magnetic fields of (a) 1 T, (b) 2 T, (c) 3 T, and (d) 4 T, respectively. The number beside each segment of data represents the measurement temperature.

be 15, 14, 13, and 13 for fields of 1, 2, 3, and 4 T, respectively. The C values presented here are obviously not strongly field dependent. It is clear that a single value of C for each field does not result in a smooth curve over a wide range of temperature, especially for the high-temperature data. In order to account for the explicit temperature dependence of the activation energy, we choose a form of temperature scaling function $G(T)$ that is compatible with the apparent temperature independence below 15 K:

$$G(T) = 1 - (T/T_x)^2, \quad (8)$$

where T_x is a characteristic temperature, which is initially taken from the magnetic irreversibility line (see Fig. 1) and slightly adjusted manually to align the high-temperature data such that a continuous curve of $U_{\text{eff}}/kG(T)$ vs M (see Fig. 8, the lower left curve of each pair) can be obtained. $G(T)$ changes slightly with temperature for $T \ll T_x$ and drops rapidly as T approaches T_x . A detailed discussion of choosing the function $G(T)$ has been given by McHenry *et al.*³¹ From our fits the T_x 's were determined to be 90, 89, 86, and 84 K for the fields of 1, 2, 3, and 4 T, respectively. The C and T_x values are listed in Table I. The curves shown in Fig. 8 with higher effective activation energies associated with lower values of M (or equivalently J) imply that, due to a faster creep rate at a temperature near the irreversibility line, significant relaxation may occur even before the measurement starts.

To investigate the effect of magnetic fields upon the effective activation energy, we have obtained a universal curve $U_{\text{eff}}(J)$, as shown in Fig. 9(b) by scaling the data of Fig. 9(a) by $H^{0.55}$. The exponent 0.55 is the value examined in the range 0.0–1.2 that gives the best fit for all the data from 5 to 50 K and 1 to 4 T. Notice that the x axis has been converted from M to J to show explicitly the current dependence of U_{eff} . Although an $\sim H^{-1}$ dependence has been previously derived using the Anderson-Kim model of the activation energy combined with the Ginzburg-Landau expressions for the coherence length, thermodynamic critical field, and depairing critical current density, etc.,^{5,6} the relation $J_c \sim H^{-0.5}$, which leads to the dependence $U_{\text{eff}} \sim H^{-0.5}$, has also been suggested for the case if flux pinning is dominated by twinning planes.^{32,33} Recently, Murakami *et al.*³⁴ have derived an expression $J \sim H^{-0.5}$ for 211 precipitates which have dimensions somewhat larger than the coherence length but still effectively pin the vortices. Such a field dependence basically agrees with what is observed in this work. The magnitude of the pinning potential is determined by the interaction between the flux lattice and de-

fect structures, and MPMG $\text{YBa}_2\text{Cu}_3\text{O}_7$ samples are usually heavily twinned and free of weak links. The twin planes in $\text{YBa}_2\text{Cu}_3\text{O}_7$ extend through the thickness of the crystal, which is parallel to the c axis and the applied field in this work, so that it is possible to have a weak field dependence, which implies higher pinning energies, if, in addition to Y_2BaCuO_5 inclusions, the twin planes also act as strong pinning centers in a certain range of temperature (especially at low temperature) and magnetic field.

The final expression for the current dependence of U_{eff} , which takes into account the nonlinear current dependence of activation energy, is then given as

$$U_{\text{eff}}(J, H) = U_i [1 - (T/T_x)^2] F(J/J_i) / H^{0.55}, \quad (9)$$

where U_i and J_i are scaling values that depend upon J/J_c .¹⁷ Figure 10 shows a log-log plot of U_{eff} vs J in which two different power-law regimes are observed. This result may imply different flux bundle sizes in the two regimes. To rationalize this, we consider the theory of collective flux creep which gives¹⁷

$$U_{\text{eff}}(J) \sim (J/J_i)^{-n}, \quad (10)$$

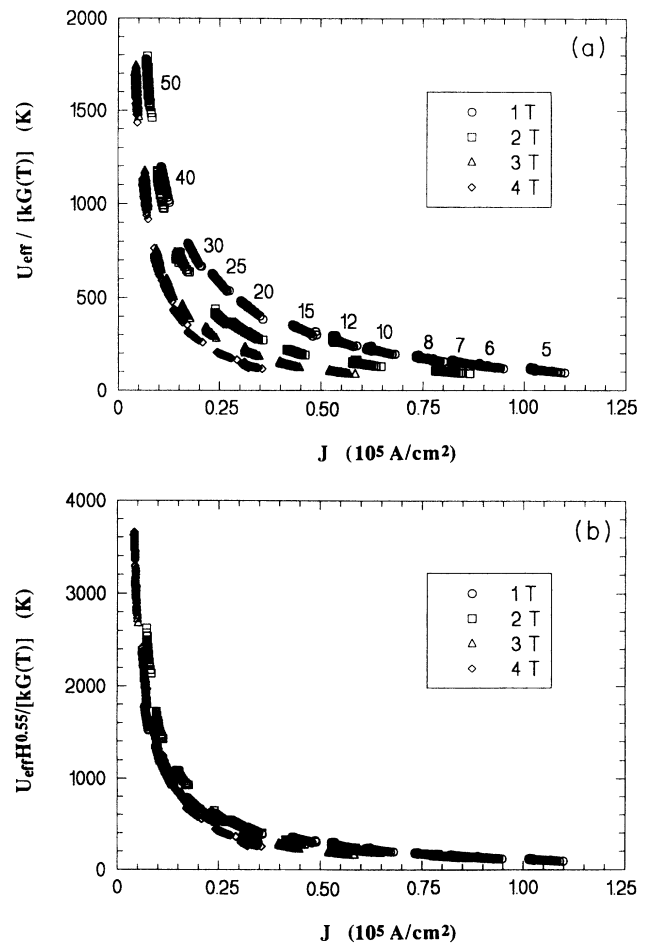


FIG. 9. Fits of (a) $U_{\text{eff}}/[kG(T)]$ vs J and (b) $U_{\text{eff}}H^{0.55}/[kG(T)]$ vs J for the data of Fig. 8 taken up to 50 K, where $G(T) = 1 - (T/T_x)^2$. The number beside each segment of data represents the measurement temperature. For clarity, some of the data at 1 T below 50 K are not included.

TABLE I. Constants and characteristic temperatures used to curve-fit the temperature dependence of U_{eff} .

H (T)	C	T_x (K)
1	15	90
2	14	89
3	13	86
4	13	84

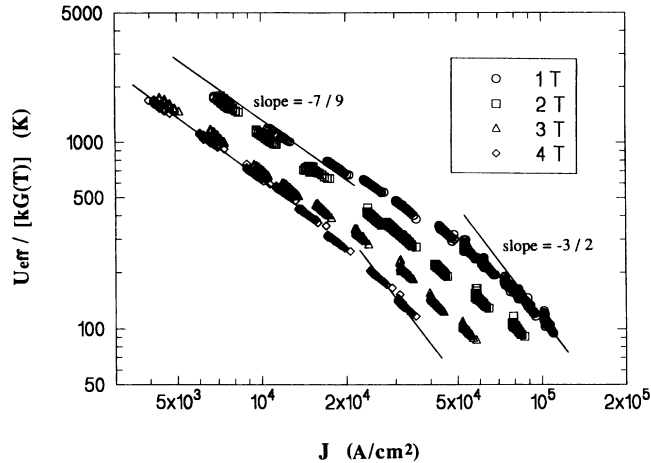


FIG. 10. Fit of $\log U_{\text{eff}}/[kG(T)]$ vs $\log J$ showing two different regimes. Solid lines are obtained from the theory of collective flux creep and drawn for comparison. The diverging behavior of U_{eff} in the low-current range indicates a vortex-glass state.

where $n = \frac{1}{7}$, $\frac{3}{2}$, and $\frac{7}{9}$ for $J \sim J_c$, $J < J_c$, and $J \ll J_c$, respectively. In Fig. 10, the solid lines are obtained from the theory of collective flux creep and drawn for comparison. Although the dependences are not exactly matched, the data do show a similarity to the theoretical predications, especially at high temperatures and high fields. In particular, both the data and the model show two regimes ($J < J_c$ and $J \ll J_c$) and a decrease in slope for smaller values of J . The diverging behavior of U_{eff} at low current density clearly suggests a vortex-glass state. Because the rapid initial relaxation becomes more important as the measuring temperature moves towards the irreversibility line, we can expect U_{eff} , which is the average value of the pinning energy, to be higher in the high-temperature range, i.e., the flux-pinning energy is strongly dependent

on the current at $J \ll J_c$. Also, there exists another regime for the relaxation data taken below 5 K. It is believed that this temperature range is in the regime near the critical state ($J \sim J_c$). However, this low-temperature behavior is still not completely understood at this moment and it will be the subject of a future publication.

IV. CONCLUSIONS

Magnetic hysteresis and relaxation measurements have been performed on a MPMG $\text{YBa}_2\text{Cu}_3\text{O}_7$ sample. Critical current densities derived from the Bean model and the sample dimensions are almost independent of the magnetic field up to 70 K. A linear relation between $\ln(\Delta M)$ and T was observed in this work, indicating that the simple linear dependence model for U_{eff} cannot correctly explain the behavior of flux creep in MPMG $\text{YBa}_2\text{Cu}_3\text{O}_7$. A universal curve of the effective pinning energy versus current density incorporating the scaling of both temperature and magnetic field, $U_{\text{eff}}(J, H) = U_i [1 - (T/T_x)^2] F(J/J_i) / H^{0.55}$, where $F(J/J_i) \sim (J/J_i)^{-n}$ and T_x near T_c , has been obtained. The current-dependent behavior of the effective pinning energy $U_{\text{eff}}(J, H)$, taking into account the unobservable flux creep occurring in the regime $J \sim J_c$ prior to the measurement of magnetic relaxation, is in qualitative agreement with the theory of collective flux creep. The model predicts three regimes ($J \ll J_c$, $J < J_c$, and $J \sim J_c$); the data in this work show similar trends to that expected for the first two regimes, and the third is expected to exist for $T < 5$ K but cannot yet be demonstrated. The values of U_{eff} diverge in the low-current region (equivalently, high-temperature range in our measurements), which indicates a vortex-glass state.

ACKNOWLEDGMENTS

This work was performed under the auspices of the United States Department of Energy, Office of Energy Management.

*Permanent address: Department of Metallurgical Engineering and Materials Science, Carnegie Mellon University, Pittsburgh, PA 15213-3890.

¹M. K. Wu, J. R. Ashburn, and C. W. Chu, *Phys. Rev. Lett.* **58**, 908 (1987).

²H. Maeda, Y. Tanaka, M. Fukutomi, and T. Asano, *Jpn. J. Appl. Phys.* **27**, L209 (1988).

³Z. Sheng and A. M. Hermann, *Nature* **332**, 138 (1988).

⁴T. T. M. Palstra, B. Batlogg, R. B. van Dover, L. F. Schneemeyer, and J. V. Waszczak, *Appl. Phys. Lett.* **54**, 763 (1989).

⁵Y. Yeshurun and A. P. Malozemoff, *Phys. Rev. Lett.* **60**, 2202 (1988).

⁶M. Tinkham, *Phys. Rev. Lett.* **61**, 1658 (1988).

⁷E. Zeldov, N. M. Amer, G. Koren, M. W. McElfresh, and R. J. Gambino, *Appl. Phys. Lett.* **56**, 680 (1990).

⁸G. M. Stollman, B. Dam, J. H. P. M. Emmen, and J. Pankert, *Physica C* **159**, 854 (1989).

⁹M. D. Lan, J. Z. Liu, and R. N. Shelton, *Phys. Rev. B* **44**, 233

(1991).

¹⁰C. Keller, H. Kupfer, A. Gurevich, R. Meier-Hirmer, T. Wolf, R. Flukiger, V. Selvamanickam, and K. Salama, *J. Appl. Phys.* **68**, 3498 (1990).

¹¹S. Jin, R. C. Sherwood, E. M. Sherwood, E. M. Gyorgy, T. H. Tiefel, R. B. van Dover, S. Nakahara, L. F. Schneemeyer, R. A. Fastnacht, and M. E. Davis, *Appl. Phys. Lett.* **54**, 584 (1989).

¹²M. P. Maley, P. J. Kung, J. Y. Coulter, W. L. Carter, G. N. Riley, and M. E. McHenry, *Phys. Rev. B* **45**, 7566 (1992).

¹³M. Ueyama, T. Hikata, T. Kato, and K.-I. Sato, *Jpn. J. Appl. Phys.* **30**, L1384 (1991).

¹⁴M. Murakami, *Mod. Phys. Lett.* **4**, 163 (1990).

¹⁵M. Murakami, M. Morita, K. Doi, and K. Miyamoto, *Jpn. J. Appl. Phys.* **28**, 1189 (1989).

¹⁶M. P. A. Fisher, *Phys. Rev. Lett.* **62**, 1415 (1989).

¹⁷M. V. Feigel'man, V. B. Geshkenbein, A. I. Larkin, and V. M. Vinokur, *Letts.* **63**, 2303 (1989).

¹⁸P. W. Anderson, *Phys. Rev. Lett.* **9**, 309 (1962).

- ¹⁹P. W. Anderson and Y. B. Kim, *Rev. Mod. Phys.* **36**, 39 (1964).
- ²⁰A. M. Campbell and J. E. Evetts, *Adv. Phys.* **21**, 199 (1972).
- ²¹M. R. Beasley, R. Labusch, and W. W. Webb, *Phys. Rev.* **181**, 682 (1969).
- ²²Y. Xu, M. Suenaga, A. R. Moodenbaugh, and D. O. Welch, *Phys. Rev. B* **40**, 10 882 (1989).
- ²³C. W. Hagen and R. Griessen, *Phys. Rev. Lett.* **62**, 2857 (1989).
- ²⁴M. V. Feigel'man, V. B. Geshkenbein, and V. M. Vinokur, *Phys. Rev. B* **43**, 6263 (1991).
- ²⁵A. P. Malozemoff and M. P. A. Fisher, *Phys. Rev. B* **42**, 6784 (1990).
- ²⁶M. P. Maley, J. O. Willis, H. Lessure, and M. E. McHenry, *Phys. Rev. B* **42**, 2639 (1990).
- ²⁷A. Umezawa, G. W. Crabtree, J. Z. Liu, H. W. Weber, W. K. Kwok, L. H. Nunez, T. J. Moran, and C. H. Sowers, *Phys. Rev. B* **36**, 7151 (1988).
- ²⁸R. Griessen, J.G. Lensink, and H. G. Schnack, *Physica C* **185-189**, 337 (1991).
- ²⁹I. A. Campbell, L. Fruchter, and R. Cabanel, *Phys. Rev. Lett.* **64**, 1561 (1990).
- ³⁰J. R. Thompson, Y. R. Sun, L. Civale, A. P. Malozemoff, M. W. McElfresh, A. D. Marwick, and F. Holtzberg (unpublished).
- ³¹M. E. McHenry, S. Simizu, H. Lessure, M. P. Maley, J. Y. Coulter, I. Tanaka, and H. Kojima, *Phys. Rev. B* **44**, 7614 (1991).
- ³²T. Matsushita and B. Ni, *IEEE Trans. Mag.* **TM-25**, 2285 (1989).
- ³³T. Matsushita, S. Funaba, Y. Nagamatsu, B. Ni, K. Funaki, and K. Yamafuji, *Jpn. J. Appl. Phys.* **28**, L1508 (1989).
- ³⁴M. Murakami, S. Gotoh, H. Fujimoto, K. Yamaguchi, N. Koshizuka, and S. Tanaka, *Supercond. Sci. Technol.* **4**, S43 (1991).